

Molecular-weight dependence of the glass transition temperature of freely-standing poly(methyl methacrylate) films

C.B. Roth^a, A. Pound, S.W. Kamp, C.A. Murray, and J.R. Dutcher^b

Department of Physics and the Guelph-Waterloo Physics Institute, University of Guelph, Guelph, Ontario, N1G 2W1 Canada

Received 17 May 2006 /

Published online: 7 September 2006 – © EDP Sciences / Società Italiana di Fisica / Springer-Verlag 2006

Abstract. We have used transmission ellipsometry to measure the glass transition temperature, T_g , of freely-standing films of atactic and syndiotactic poly(methyl methacrylate) (PMMA). We have prepared films with different molecular weights, MW, ($159 \times 10^3 < M_w < 1.3 \times 10^6$) and film thicknesses, h , ($30 \text{ nm} < h < 200 \text{ nm}$). For the high-MW ($M_w > 509 \times 10^3$) atactic PMMA films, we find that T_g decreases linearly with decreasing h , which is qualitatively similar to previous results obtained for high-MW freely-standing polystyrene (PS) films. However, the overall magnitude of the T_g reduction is much less (by roughly a factor of three) for the high-MW freely-standing PMMA films than for freely-standing PS films of comparable MW and h . The observed differences between the freely-standing PMMA and PS film data suggest that differences in chemical structure determine the magnitude of the T_g reduction and we discuss the possible origins of these differences. Our analysis of the MW-dependence of the T_g reductions suggests that the mechanism responsible for the MW-dependent T_g reductions observed in the high-MW freely-standing films is different than that responsible for the MW-independent T_g reductions observed in the low-MW freely-standing and supported films.

PACS. 36.20.-r Macromolecules and polymer molecules – 36.20.Cw Molecular weights, dispersity – 64.70.Pf Glass transitions – 65.40.De Thermal expansion; thermomechanical effects

1 Introduction

The effects of confinement and free surfaces on the dynamics of polymers in thin films have been studied extensively since the original observation of reductions in T_g with decreasing film thickness in thin polystyrene (PS) films [1,2]. The progress achieved in this area of research is considerable and has been described in detail in recent reviews [3–6]. For the case of supported PS films, the dependence of T_g on film thickness h has been measured using many different experimental techniques, including ellipsometry, dielectric spectroscopy, X-ray reflectivity, positron annihilation spectroscopy, fluorescence spectroscopy and local thermal analysis (see Ref. [4] for details). The T_g values obtained using all of these techniques are in quantitative agreement showing no significant dependence on molecular weight (MW) [7], and the

dependence on h can be described by [1]

$$T_g(h) = T_g^{\text{bulk}} \left[1 - \left(\frac{a}{h} \right)^\delta \right], \quad (1)$$

where T_g^{bulk} is the bulk value of T_g .

One particularly striking result, which is yet to be understood in detail, is the observation of very large reductions of T_g in very thin, freely-standing PS films using Brillouin light scattering and ellipsometry [8–13]. For all MW values, the reductions in T_g at a given film thickness were much larger for freely-standing PS films than for supported films of the same thickness. In addition, the dependence of T_g on film thickness h for freely-standing PS films showed an interesting crossover in behavior between low and high MW values. For low MW values ($M_w < 370 \times 10^3$), the $T_g(h)$ data are well described by the equation used to fit the supported PS film data, equation (1), with no measurable MW-dependence and a T_g reduction at a given value of h that is twice as large as that observed for a supported PS film of the same thickness [14]. For high MW values (six different M_w values greater than 370×10^3 , ranging from 575×10^3 to 9.1×10^6), the results differed *qualitatively* in several ways from those obtained

^a Present address: Department of Chemical and Biological Engineering, Northwestern University, Evanston, IL 60208-3120, USA.

^b e-mail: dutcher@physics.uoguelph.ca

for supported and low-MW freely-standing PS films: 1) the magnitude of the overall $T_g(h)$ reduction was much larger than for supported PS films, *e.g.* a 70 °C reduction for freely-standing films of $h \simeq 30$ nm compared to a 7 °C reduction for supported films of $h \simeq 30$ nm; 2) the T_g values decreased linearly with decreasing film thickness below a threshold film thickness h_0 , characterized by the equation

$$T_g = \begin{cases} T_g^{\text{bulk}} + \alpha(h - h_0), & h < h_0 \\ T_g^{\text{bulk}}, & h > h_0; \end{cases} \quad (2)$$

and 3) the $T_g(h)$ behavior was found to depend systematically on MW, *e.g.* the slope α in equation (2) that characterizes the linear decrease in T_g with decreasing film thickness increased monotonically with increasing MW [9,13]. By fitting straight lines to the $T_g(h)$ data for each MW value (cf. Eq. (2)) and extrapolating the best-fit straight lines to higher temperatures, all six of the straight lines, one for each MW value, intersected at a single point (h^* , T_g^*). The existence of the common intersection point allowed the construction of a universal scaling plot of the film thickness dependence of the T_g reductions in which all of the reduced T_g values measured for different h and MW values collapsed onto a single line [13].

The dependence of the $T_g(h)$ values on MW observed for high-MW freely-standing PS films is surprising because the length scale associated with the glass transition, corresponding to cooperative segmental dynamics, in bulk samples is of the order of only a few hundreds of monomers [15], which is much less than the lateral extent of the chain, and the cooperative segmental dynamics in bulk have no measurable dependence on MW. In thin polymer films, the dynamics on much longer length scales can be effectively decoupled from segmental dynamics, as shown recently by comparing T_g measurements on freely-standing PS films, for which large T_g reductions are observed, with measurements of film rupture and hole growth in these films, which probe the motion of entire polymer chains and can be understood in terms of bulk dynamics [4,16,17]. This discrepancy between dynamics on different length scales in thin polymer films has also been observed in ellipsometric measurements of T_g and measurements of interface healing in PS bilayer films [18].

To date, a satisfactory explanation for the unusual and complex MW-dependence of the $T_g(h)$ behavior of high-MW freely-standing PS films has not been found. Currently the only theoretical model that predicts a MW-dependence for T_g reductions is due to de Gennes [19,20]. He proposed a new mode of mobility, a “sliding mode”, which becomes the dominant mechanism for segmental mobility in very thin polymer films allowing for motion of chain segments within the tube between points of the tube at the free surfaces of the film: either between points on the same free surface (*loops*), or between points on the two opposite free surfaces (*bridges*). de Gennes proposed that the sliding mode becomes dominant as the polymer film thickness is decreased to values comparable to the overall size of the polymer coils. Although this model can provide a qualitative explanation for the observed linear

decrease in T_g with decreasing film thickness, with a MW-dependence that is similar to that observed, full quantitative agreement with the experimental data is still lacking.

Theoretical efforts for the $T_g(h)$ results in supported and low-MW freely-standing films have focused on the concept of increased segmental mobility at the free surface of the films, and mechanisms by which the increased mobility could be propagated deeper into the films [14,21–26]. Such an approach seems valid since numerous experimental studies have demonstrated increased mobility at the free surface [4], which is observed to result in a gradient in T_g as a function of depth until bulk T_g is recovered some tens of nanometers from the free surface [27]. Several models have been proposed to describe the supported and low-MW freely-standing film $T_g(h)$ data: a layer model proposed by Forrest and Mattsson [14], a percolation model proposed by Long and coworkers [21,22], a viscoelastic model proposed by Herminghaus and coworkers [23,24], and a coupling model proposed by Ngai [25,26].

Recently T_g measurements were performed on high-MW freely-standing films of a second polymer, poly (methyl methacrylate) (PMMA), using transmission ellipsometry [28]. PMMA was selected because it has root-mean-square end-to-end distance R_{ee} and bulk T_g values that are similar to those for PS of comparable molecular weight. These results demonstrated that for atactic PMMA of a single MW value, $M_w = 790 \times 10^3$, T_g decreased linearly with decreasing film thickness, which was qualitatively similar to freely-standing PS films, but the magnitude of the T_g reduction was much less for the PMMA films, *e.g.* for freely-standing films with thickness $h = 40$ nm, a T_g reduction of ~ 15 °C was observed for PMMA of $M_w = 790 \times 10^3$ which is much less than the T_g reduction of ~ 55 °C observed for PS of $M_w = 767 \times 10^3$ [28]. Since these measurements were performed on freely-standing films, these differences cannot be attributed to specific interactions between the polymer chains and an underlying substrate as was argued previously for differences in $T_g(h)$ data of supported PS and PMMA films on silicon substrates [1,2]. Instead, it was reasoned that the differences in the magnitude of the T_g reductions between the high-MW freely-standing PS and PMMA films must be due to the inherent differences in chemical structure between the two polymers [28].

The results presented in this paper extend the initial study of freely-standing films of atactic PMMA with a single value of $M_w = 790 \times 10^3$ to investigate the MW-dependence of the $T_g(h)$ behavior for freely-standing PMMA films. We present the results of $T_g(h)$ measurements on freely-standing films with two other high MW values of atactic PMMA, $M_w = 509 \times 10^3$ and 1300×10^3 , as well as on freely-standing films with a much smaller MW value, $M_w = 159 \times 10^3$, of syndiotactic PMMA. For films with high MW values ($M_w > 509 \times 10^3$), we observed the same qualitative dependence on film thickness as was observed for high-MW freely-standing PS films: a linear decrease in T_g with decreasing film thickness, and a monotonic dependence of the $T_g(h)$ results on MW. However, the magnitude of the T_g reductions observed for

Table 1. Weight average molecular weight M_w , polydispersity index M_w/M_n , and root-mean-square end-to-end distance R_{ee} values for the PMMA used in the present study. The glass transition temperature T_g^{bulk} , as measured using ellipsometry for films > 300 nm, is given along with the best-fit values of the slope α and threshold thickness h_0 obtained by fitting equation (2) to the data shown in Figure 2.

PMMA tacticity	$M_w (\times 10^3)$	M_w/M_n	R_{ee} (nm)	T_g^{bulk} ($^{\circ}\text{C}$)	α ($^{\circ}\text{C}/\text{nm}$)	h_0 (nm)
79% syndiotactic	159	1.09	27	118	–	–
atactic	509	< 1.11	48	115	0.156 ± 0.026	98 ± 6
atactic	790	< 1.11	60	110	0.259 ± 0.025	95 ± 3
atactic	1300	< 1.11	77	115	0.352 ± 0.041	97 ± 2

the freely-standing PMMA films is observed to be much less than that for freely-standing PS films of comparable MW value. The analysis of the results for the high-MW freely-standing PMMA films suggests that no T_g reductions should be observed for $M_w < M_w^* = 236 \times 10^3$ due to the mechanism which causes the MW-dependent T_g reductions in high-MW freely-standing polymer films. However, for freely-standing PMMA films with $M_w = 159 \times 10^3 < M_w^*$, we observed T_g reductions that were comparable in magnitude to those observed for the high MW values, with a $T_g(h)$ behavior that was similar to that observed for supported and low-MW freely-standing PS films, as described by equation (1). The results of the present study suggest that the mechanism responsible for the T_g reductions in the high-MW freely-standing films is different than that responsible for the low-MW freely-standing and supported films. We discuss the structural and dynamical differences between PS and PMMA that could explain the observed differences in the overall magnitude of the T_g reductions.

2 Experiment

Thin films of atactic and syndiotactic poly(methyl methacrylate) were prepared by spincoating dilute solutions of monodisperse polymer dissolved in toluene. Solution concentrations ranging from 1% to 6% PMMA by mass were spun onto freshly-cleaved mica at spin speeds between 1500 and 5500 rpm which produced film thicknesses h ranging from 20 to 307 nm. The PMMA films supported on the mica substrates were annealed under vacuum at $T = 125$ $^{\circ}\text{C}$ or 140 $^{\circ}\text{C}$ for 12 h to remove residual solvent, and then cooled at 1 $^{\circ}\text{C}/\text{min}$ to room temperature, to produce a well-defined and reproducible thermal history. A water transfer technique [9] was used to transfer the PMMA films from the mica substrates onto 1 cm^2 nylon sample holders containing 4 or 5 mm diameter holes, creating freely-standing PMMA films. Nylon sample holders were used because they prevented the buildup of in-plane stress in the polymer film upon heating and cooling due to differences in thermal expansion between the sample and the holder [13]. Pieces of the same PMMA films were also transferred onto clean silicon wafers for the determination of the initial film thickness to within ± 1 nm using reflection ellipsometry. Table 1 lists the weight average molecular weight M_w , polydispersity index M_w/M_n , root-mean-square end-to-end distance R_{ee} [29], and the glass transition temperature T_g^{bulk} of very thick films with

$h > 300$ nm for the PMMA samples studied. The small differences in T_g^{bulk} between the samples result from slight variations in the tacticity [30].

Transmission ellipsometry was used to determine the glass transition temperature T_g of the freely-standing PMMA films by measuring the temperature dependence of the film thickness in the melt and glassy states. The measured ellipsometric angles, P (polarizer) and A (analyzer), collected over the range of temperatures T from 85 to 130 $^{\circ}\text{C}$, were converted to film thickness h and index of refraction n assuming an isotropic index of refraction of the polymer film [31]. The $h(T)$ and $n(T)$ values for each cooling and heating cycle were fit to a function of the form

$$w_i \left(\frac{M_i - G_i}{2} \right) \ln \left[\cosh \left(\frac{T - T_g}{w_i} \right) \right] + (T - T_g) \left(\frac{M_i - G_i}{2} \right) + c_i, \quad i = h, n \quad (3)$$

to obtain a T_g value for each thermal cycle. Equation (3) is an empirical equation we have used previously to fit the temperature dependence of ellipsometry data measured for freely-standing polystyrene films [13], which is derived by integrating an assumed $\tanh(T)$ profile for the transition between the thermal expansion coefficients in the melt and glassy states. In equation (3), M_i and G_i are the dh/dT and dn/dT slope values of the melt and glassy states, respectively, w_i is the width of the transition, and c_i is the value of the film thickness or index of refraction at $T = T_g$. We used this equation to determine T_g , instead of the intersection point of two independent linear fits to the data in the temperature ranges above and below T_g , to avoid the subjectivity of choosing the range of temperatures corresponding to the linear regions in the data at temperatures above and below T_g . During the fitting process, the width of the transition w_i was held fixed at 2 $^{\circ}\text{C}$ which was found to provide excellent fits to the data in all cases, as was observed in reference [13] for the freely-standing PS films. Nonlinear least-squares fits to equation (3) were performed on both the $h(T)$ and $n(T)$ data from three to five thermal (heating and cooling) cycles that were performed on each film at a heating/cooling rate of 0.5, 1.0, or 2.0 $^{\circ}\text{C}/\text{min}$. The T_g value for the film was taken to be the average value calculated from all of the thermal cycles. We observed no systematic differences between T_g values obtained on successive temperature ramps, and no differences between T_g values measured using the slightly different heating and cooling rates.

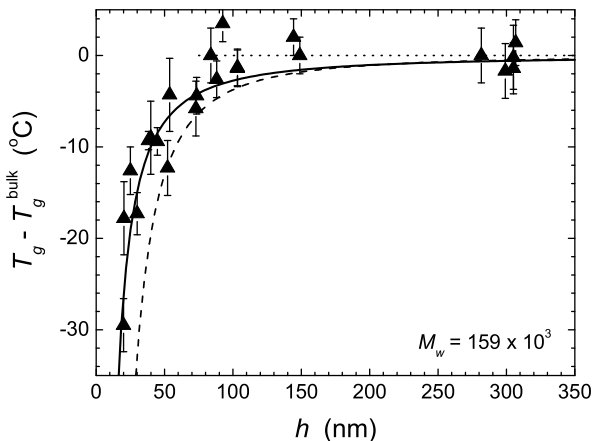


Fig. 1. Plot of $T_g - T_g^{\text{bulk}}$ versus film thickness h for low-MW freely-standing PMMA films with $M_w = 159 \times 10^3$ (symbols). The solid curve was calculated using equation (1) and the best-fit parameter values of $a = 2.9$ nm and $\delta = 1.4$. The dashed curve was calculated using equation (1) and the parameter values of $a = 7.8$ nm and $\delta = 1.8$, obtained as the best fit to the low $M_w < 370 \times 10^3$ freely-standing PS film data from reference [12].

The ellipsometry measurements were performed using a custom-built, single wavelength ($\lambda = 632.8$ nm), self-nulling ellipsometer in transmission mode [13]. Relative measurements of the ellipsometric angles P and A used to determine a null in the light intensity at the detector are accurate to within $\pm 0.001^\circ$. The measurements were performed using an angle of incidence θ_i approximately equal to the Brewster angle for PMMA, $\theta_B = 56^\circ$. At the beginning of each ellipsometry experiment, the temperature was increased rapidly at a rate of $5^\circ\text{C}/\text{min}$ from room temperature to a temperature of $T = 110^\circ\text{C}$. At this elevated temperature, the sample chamber was flushed with approximately 30 liters of room temperature dry nitrogen gas, with both sides of the freely-standing film exposed to the nitrogen gas, for typically 30 s to remove any water vapor in the chamber [32]. This procedure was performed because water can act as a plasticizer in PMMA which reduces the T_g value [33]. Following the gas flushing, the temperature was allowed to equilibrate at 110°C for 10 minutes before the temperature was further increased to a temperature that was at least 20°C greater than T_g to begin the measurement of T_g upon cooling. Nitrogen gas flushing was not performed during the ellipsometry measurements because the gas flow causes vibrations of the freely-standing films which degrades the ellipsometry measurement.

3 Results

For all of the freely-standing PMMA films (see Tab. 1), the measured values of the glass transition temperature T_g were observed to decrease with decreasing film thick-

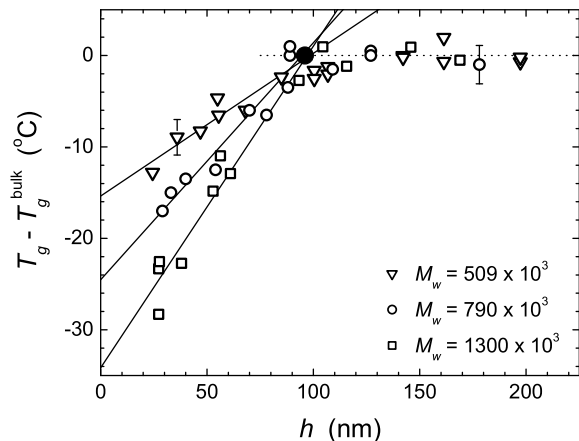


Fig. 2. Plot of $T_g - T_g^{\text{bulk}}$ versus film thickness h for high-molecular-weight freely-standing PMMA films of $M_w = 509 \times 10^3$ (inverted triangles), $M_w = 790 \times 10^3$ (circles), and $M_w = 1300 \times 10^3$ (squares). The solid lines were calculated as the best fit of equation (2) to the data for $h < 100$ nm. Representative error bars are also indicated for both thick and thin films. The highlighted intersection point (solid circle) of the three solid lines corresponds to $h^* = (96 \pm 8)$ nm and $T_g^* = (T_g^{\text{bulk}} \pm 2)^\circ\text{C}$, as described in the text.

ness h for $h < 100$ nm. In Figures 1 and 2 we plot $(T_g - T_g^{\text{bulk}})$ as a function of film thickness for the low-molecular-weight ($M_w = 159 \times 10^3$), and high-molecular-weight ($509 \times 10^3 < M_w < 1300 \times 10^3$) freely-standing PMMA films, respectively. Each data point represents the T_g value measured for a different film and representative error bars are shown for a thick and thin film in Figure 2. The quantity $(T_g - T_g^{\text{bulk}})$ is plotted in Figures 1 and 2 to account for the differences in T_g^{bulk} due to slight variations in tacticity between the different MW samples (see Tab. 1). The same ordinate scale is used in Figures 1 and 2, indicating that the overall magnitude of T_g reductions with decreasing film thickness h is similar for the low- and high-MW freely-standing PMMA films.

In Figure 1, the measured T_g values for the low-MW freely-standing PMMA films are shown, as well as a solid curve that was calculated as the best fit of the data to equation (1) using the following parameter values: $a = 2.9$ nm and $\delta = 1.4$. For comparison, a dashed curve is also shown in Figure 1 corresponding to the best fit of the low-MW freely-standing PS film data from reference [12] to equation (1) using $a = 7.8$ nm and $\delta = 1.8$. We find that the T_g reductions observed for the low-MW freely-standing PMMA films are similar in magnitude to those observed for the low-MW freely-standing PS films with a slight decrease in the size of the T_g reduction, *e.g.* for a film thickness of $h = 40$ nm, the T_g reduction for low-MW freely-standing PMMA films is $\sim 10^\circ\text{C}$ compared to a T_g reduction of $\sim 20^\circ\text{C}$ for low-MW freely-standing PS films.

In Figure 2, we plot the $T_g(h)$ data measured for the high-MW freely-standing PMMA films with different MW values. We find that, for each MW value, T_g decreases

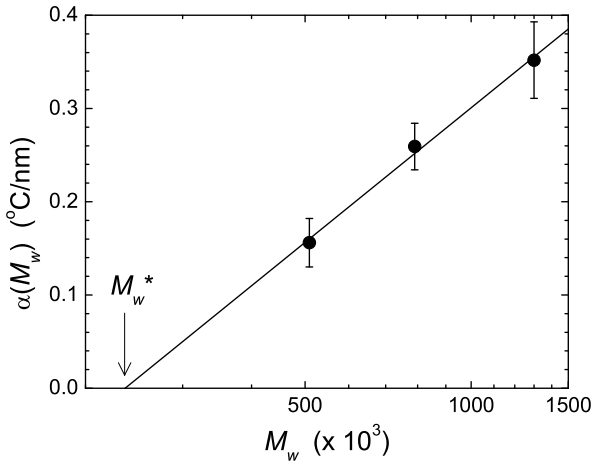


Fig. 3. The slope α characterizing the linear decrease in T_g with decreasing h plotted as a function of molecular weight M_w (cf. Eq. (2)). For the parameterization given in equation (5), the best-fit values of the fitting parameters are $b = (0.21 \pm 0.01) \text{ }^\circ\text{C/nm}$ and $M_w^* = (236 \pm 25) \times 10^3$, which is indicated by a vertical arrow as the M_w value for which $\alpha = 0$.

linearly with decreasing film thickness. For a given film thickness h , films with larger MW have larger reductions in T_g , *e.g.* for a thickness of $h = 30$ nm, a freely-standing PMMA film with $M_w = 1300 \times 10^3$ has a reduction in T_g of 23°C compared to a T_g reduction of only 10°C for a freely-standing PMMA film with $M_w = 509 \times 10^3$. We have fit the high-MW freely-standing PMMA data shown in Figure 2 to equation (2) and we find that the best-fit value of the slope α that characterizes the linear decrease in T_g with decreasing film thickness increases monotonically with increasing molecular weight (see Tab. 1). Qualitatively, this is the same behavior that was observed for high-MW freely-standing PS films [13]. However, the overall magnitude of the T_g reductions observed for the high-MW freely-standing PMMA films is much less than that observed for high-MW freely-standing PS films, as discussed below in more detail.

Remarkably, we find that the best straight-line fits of the reduced T_g data for high-MW freely-standing PMMA films ($h \lesssim 100$ nm) intersect at a common point (h^*, T_g^*). This behavior was first observed for high-MW freely-standing PS films [13]. The values of h^* for the two polymers are similar: 103 ± 1 nm for PS and 96 ± 8 nm for PMMA. This suggests that the length scale at which T_g reductions are observed is comparable for both polymers. The relevance of a length scale which is ~ 100 nm to the glass transition is not presently understood, but it is found for a variety of thin-film polymers that T_g reductions or deviations from bulk dynamics are observed for film thicknesses $h \lesssim 100$ nm [4]. Ellison and Torkelson have suggested that such a large length scale of tens of nanometers may be required to contain the full breadth of the distribution of cooperative relaxation dynamics in polymers near T_g [27]. The value of T_g^* , however, is markedly different

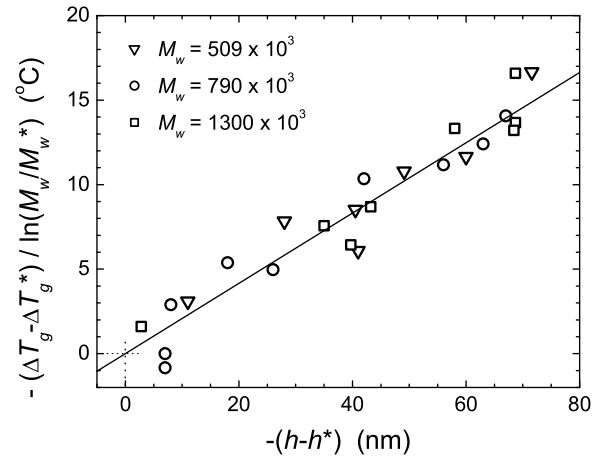


Fig. 4. Scaling plot showing the collapse of all of the reduced T_g data measured for thicknesses $h < 100$ nm for high-MW freely-standing PMMA films: $M_w = 509 \times 10^3$ (inverted triangles), $M_w = 790 \times 10^3$ (circles), and $M_w = 1300 \times 10^3$ (squares). Based on equations (4) and (5) in the text, $-(\Delta T_g - \Delta T_g^*) / \ln(M_w/M_w^*)$ versus $-(h - h^*)$ is plotted using the values of h^* , T_g^* , and M_w^* given in the captions of Figures 2 and 3, and the straight solid line has a slope of b determined from the fit in Figure 3 and is constrained to pass through the origin.

for the two polymers: $(T_g^{\text{bulk}} + 53^\circ\text{C}) \pm 2^\circ\text{C}$ for PS, and $T_g^{\text{bulk}} \pm 2^\circ\text{C}$ for PMMA. A previous analysis for the freely-standing PS films noted that the value of $T_g^* = 150^\circ\text{C}$ was similar to the temperature at which the α and β relaxation modes split, $T_{\alpha\beta} \sim 150^\circ\text{C}$ for PS [3]. However, this is clearly not the case for PMMA which has $T_g^* = T_g^{\text{bulk}}$ and $T_{\alpha\beta} \simeq 140^\circ\text{C} - 150^\circ\text{C}$ for PMMA with 70%–80% syndiotactic content [34]. The substantially lower value of T_g^* for PMMA could be because h^* has the same characteristic length scale and the magnitude of the T_g reductions are smaller overall for PMMA relative to PS. It is nonetheless intriguing that the $T_g(h)$ data obtained for different MW values exhibit common intersection points for both high-MW freely-standing PS and PMMA films.

The existence of the common intersection point in Figure 2 allows a straightforward parameterization of the MW-dependence of the T_g reductions. The reduced T_g values can be expressed as

$$(T_g - T_g^*) = \alpha(M_w)(h - h^*), \quad (4)$$

where the magnitude of the T_g reductions is characterized by the MW-dependent slope parameter $\alpha(M_w)$. In Figure 3 we plot α versus M_w for freely-standing PMMA films with the three high MW values used in the present study. As for the high-MW freely-standing PS films [13], we parameterize the MW-dependent slope parameter as

$$\alpha(M_w) = b \ln(M_w/M_w^*), \quad (5)$$

which allows us to determine values for $b = (0.21 \pm 0.01) \text{ }^\circ\text{C/nm}$ and $M_w^* = (236 \pm 25) \times 10^3$. This parameterization allows us to create a universal scaling plot

in which all of the reduced T_g data collapse onto a single line. The universal scaling plot is shown in Figure 4 in which $-(\Delta T_g - \Delta T_g^*)/\ln(M_w/M_w^*)$ is plotted *versus* $-(h - h^*)$ for all of the high-MW freely-standing PMMA film data with $h < 100$ nm using $(h^*, T_g^*) = (96 \text{ nm}, T_g^{\text{bulk}})$ and $M_w^* = 236 \times 10^3$. The solid line has a slope of $b = 0.21^\circ\text{C}/\text{nm}$ and is constrained to pass through the origin. We find that the parameterization specified by equations (4) and (5) describes the reduced $T_g(h, M_w)$ freely-standing PMMA film data well. The scatter in the reduced PMMA data relative to the solid line in Figure 4 has a standard deviation of 1.4°C compared to a standard deviation of 0.6°C for the data shown in Figure 7 of reference [13] for freely-standing PS films.

The values of b and M_w^* obtained from the freely-standing PMMA film data are substantially different from those obtained from the freely-standing PS data. The value of b is a measure of the overall magnitude of the T_g reduction: for freely-standing PMMA films, the value of b is roughly one-third ($b = 0.21^\circ\text{C}/\text{nm}$) of that for freely-standing PS films ($b = 0.70^\circ\text{C}/\text{nm}$) [13]. This demonstrates, as was shown in reference [28], that the overall magnitude of the T_g reduction in high-MW freely-standing PMMA films is much less than that of freely-standing PS films of comparable MW. M_w^* is the M_w value for which the slope $\alpha(M_w) = 0$, which implies that, for freely-standing PMMA films with $M_w < M_w^*$, no T_g reductions should be observed due to the mechanism which causes the MW-dependent T_g reduction in high-MW freely-standing polymer films. For the freely-standing PS films, a small value of $M_w^* = 69 \times 10^3$ was obtained which is approximately four times the entanglement molecular weight M_e . Preparing freely-standing films with such low MW values is very difficult since the films are typically damaged by the water transfer process. However, for the freely-standing PMMA films, we obtain $M_w^* = 236 \times 10^3$ which is large enough to allow the preparation of high-quality freely-standing films with $M_w < M_w^*$. In the present study, we have measured the film thickness dependence of T_g for a molecular weight $M_w = 159 \times 10^3 < M_w^*$. As discussed above (see Fig. 1), we observed T_g reductions for the $M_w = 159 \times 10^3$ films with a $T_g(h)$ -dependence that was described very well by equation (1), which is the same functional form that describes the T_g reductions observed in low-MW freely-standing PS films and supported polymer films. This provides strong evidence that the mechanism responsible for the T_g reductions in the low-MW freely-standing and supported films is different than that responsible for the T_g reductions in the high-MW freely-standing films.

4 Discussion

Differences in the magnitude and sign of T_g reductions observed for thin films of different polymers supported on substrates are typically attributed to specific interactions between the polymer and the substrate. Although these effects are certainly important and may dominate in the

case of supported films, the comparison of the results reported in the present paper for freely-standing PMMA films with those obtained previously for freely-standing PS films indicates that there are also inherent differences in the overall magnitude of the T_g reductions between polymers with different chemical structures. This is consistent with the results of a recent study on poly(4-tert-butylstyrene) (PTBS) which showed that the size of the side group can have large effects on the overall magnitude of the T_g reduction in supported films [7].

We now consider the specific differences in chemical structure of PS and PMMA that might give rise to the observed quantitative difference in the T_g reductions. The strong influence of the free surface on the mobility of polymer segments in the film has been well established [4, 27]. Therefore, it is reasonable to consider that there might exist a difference in the interaction of the PS and PMMA side groups with air that could account for the observed difference in the overall magnitude of the T_g reductions. However, this seems unlikely since the surface tensions of PS and PMMA are essentially identical, particularly at temperatures near T_g [35]. Surface tension tends to strongly hinder the motion of segments out of the plane of the film, and because of this, computer simulations often model the free surface simply as a repulsive wall [6]. Motions parallel to the plane of the film are likely enhanced at the free surface due to the reduced number of neighboring chains that segments at the free surface slide past. However, there is no *a priori* reason why this might affect PS more than PMMA.

Unlike PS, PMMA has strong polar units which likely result in interactions between neighboring chains that are stronger than in PS. This may explain why atactic PMMA has a bulk T_g value that is slightly larger than that of atactic PS even though the two polymer chains have similar persistence lengths [36–38]. However, it is not clear why an increase in the interaction strength between neighboring chains might lead to $T_g(h)$ reductions with a smaller slope. In the context of de Gennes' sliding mode [19, 20], a theoretical model proposed for the T_g reductions in high-MW freely-standing PS films, a stronger interaction between neighboring PMMA chains could imply a larger energy barrier for the sliding motion to occur [39], which could conceivably lead to a decrease in the slope of the T_g reduction.

For PMMA, the motions associated with α - and β -relaxations are more complex than for other polymers due to its molecular structure. It is well known that PMMA exhibits significantly different T_g values with changes in tacticity: the T_g value for bulk isotactic PMMA is $\sim 60^\circ\text{C}$, whereas the T_g value for bulk syndiotactic PMMA is $\sim 150^\circ\text{C}$ [40]; the T_g value for bulk atactic PMMA, which typically has $\sim 60\%$ syndiotactic content, ranges from 110°C to 115°C . In 1981, O'Reilly and Mosher identified infra-red (IR) absorption peaks associated with backbone motion and backbone-plus-side-chain motion in PMMA [41]. Subsequently, Grohens *et al.* used the ratio of intensities of these IR peaks to show that a cooperative interaction exists between the side-chain and

backbone motions in isotactic PMMA, and to a lesser extent in syndiotactic PMMA [42]. They interpreted their results by suggesting that a conformational transition of the backbone in isotactic PMMA may be energetically compensated by a side-chain rotation, and vice versa. Rotational isomeric state (RIS) calculations of PMMA by Sundararajan [43] and Vacatello and Flory [44] showed that the change in conformational energy of the backbone and side-group motions were similar in isotactic PMMA, but not in syndiotactic PMMA, suggesting that an exchange in energy between backbone and side-group motions could occur in isotactic PMMA. This unusual linkage between the side-chain and backbone motions is believed to explain why the T_g value of isotactic PMMA is so much lower than that of syndiotactic PMMA [42]. It has been proposed that the coupling of the β -process to the backbone motions is a result of the asymmetric geometry of the ester side group in PMMA which causes steric problems with adjacent segments after 180° flips of the side group [45,46]. This interpretation is based on 2D NMR spectroscopy measurements of atactic PMMA showing that the backbone undergoes 20° root-mean-square amplitude rotations around the local chain axis due to steric constraints when the carboxyl plane (O=C-O) of the ester side group undergoes 180° flips [45,46]. This rocking motion of the backbone in PMMA caused by side-group flips, which is also present below T_g , causes higher mobility of the backbone above T_g compared to other polymers such as PS. For example, at a temperature $T^* = T/T_g = 1.05$, the mean correlation time for PS is 12 ms, which is larger by two orders of magnitude than that for PMMA (0.15 ms), even though PS and PMMA have similar bulk T_g values [46]. In addition, the width of the distribution of correlation times for PS is larger by an order of magnitude than that for PMMA. Based on all of these results it appears that an exchange of energy can occur between backbone (α -) and side-chain (β -) motions in PMMA. This coupling between α - and β -motions is most prominent in isotactic PMMA, but exists to some degree in all tacticities of PMMA since meso (isotactic) dyads are present at some level in all PMMA chains.

How could this unusual coupling between the backbone and side-chain motions of PMMA affect the magnitude of the T_g reductions? We propose that as the film thickness decreases, resulting in a decrease in T_g and a corresponding increase in the motion associated with the α -modes, more energy is present in the α -modes which can be transferred to the β -modes. To better illustrate this idea, we consider the simplest possible case in which at a given temperature a certain fixed percentage of the total thermal energy present in the α - and β -modes manifests itself as motion associated with the β -modes. In reality, there will be a continuous exchange of energy from the α - to β -modes, and vice versa, but this exchange will quickly reach a steady state in which a certain percentage of the available thermal energy will be contained in the β -modes while the remaining energy will be contained in the α -modes. We are ignoring all other motions in the system since they do not interact. Given that PMMA and PS have similar T_g^{bulk}

and R_{ee} values it is reasonable to suppose that, in the absence of this unusual α - β coupling, PMMA would have a $T_g(h)$ reduction similar to that for PS. The transfer of a fixed percentage of the α -mode energy to the β -modes would result in less energy to be dissipated by the α -modes at a given temperature, which would result in a decrease of the slope of the $T_g(h)$ data. At every thickness h , the T_g reduction in PMMA would be reduced by a certain percentage from the observed T_g reduction in a PS film of equivalent thickness and molecular weight. It is as if the β -modes “siphon” off more energy from the α -modes for thinner PMMA films, leading to smaller T_g reductions at a given film thickness than that observed for PS. Further measurements on freely-standing films of a high-molecular-weight isotactic PMMA would aid in elucidating this idea.

5 Conclusions

We have used transmission ellipsometry to measure the glass transition temperature T_g as a function of film thickness h for freely-standing PMMA films with four different molecular-weight values ($159 \times 10^3 < M_w < 1300 \times 10^3$). We compare our findings with previous measurements obtained using the same experimental technique on freely-standing PS films. For the high-MW PMMA films ($509 \times 10^3 < M_w < 1300 \times 10^3$), we find that T_g decreases linearly with decreasing film thickness h in qualitative agreement with the high-MW freely-standing PS films previously measured. However, we find that the overall magnitude of the T_g reduction in the high-MW freely-standing PMMA films is much less (by roughly a factor of three) than that observed in freely-standing PS films of comparable molecular weight. Since there are no specific polymer-substrate interactions for freely-standing films that could lead to differences in T_g between the two polymers, this result suggests that the observed differences in T_g with decreasing film thickness between the two polymers are due to differences in the chemical structure and dynamics of the polymers.

By characterizing the MW-dependence of the T_g reductions for the high-MW freely-standing PMMA films, we have identified a molecular-weight value $M_w^* = 236 \times 10^3$ below which no T_g reduction should be observed due to the mechanism responsible for MW-dependent T_g reductions. The value of M_w^* corresponds to the MW value at which the slope $\alpha(M_w)$, characterizing the linear reduction in T_g (Eq. (2)), is equal to zero. For freely-standing PMMA films with $M_w = 159 \times 10^3 < M_w^*$, we observe $T_g(h)$ reductions that are comparable in magnitude to those observed for the high-MW films and which follow a different functional form (Eq. (1)) corresponding to that used previously to fit the MW-independent $T_g(h)$ behavior observed for low-MW freely-standing PS and supported polymer films. These results suggest that the mechanism responsible for the MW-dependent T_g reductions observed in the high-MW freely-standing films is different than that responsible for the MW-independent T_g reductions observed in the low-MW freely-standing and supported films.

Financial support from the Natural Sciences and Engineering Research Council (NSERC) of Canada and the Province of Ontario (PREA program) is gratefully acknowledged.

References

- J.L. Keddie, R.A.L. Jones, R.A. Cory, *Europhys. Lett.* **27**, 59 (1994).
- J.L. Keddie, R.A.L. Jones, R.A. Cory, *Faraday Discuss.* **98**, 219 (1994).
- J.A. Forrest, K. Dalnoki-Veress, *Adv. Colloid Interface Sci.* **94**, 167 (2001).
- C.B. Roth, J.R. Dutcher, in *Soft Materials: Structure and Dynamics*, edited by J.R. Dutcher, A.G. Marangoni (Marcel Dekker, 2004).
- M. Alcoutlabi, G.B. McKenna, *J. Phys.: Condens. Matter* **17**, R461 (2005).
- J. Baschnagel, F. Varnik, *J. Phys.: Condens. Matter* **17**, R851 (2005).
- C.J. Ellison, M.K. Mundra, J.M. Torkelson, *Macromolecules* **38**, 1767 (2005).
- J.A. Forrest, K. Dalnoki-Veress, J.R. Stevens, J.R. Dutcher, *Phys. Rev. Lett.* **77**, 2002; 4108 (1996).
- J.A. Forrest, K. Dalnoki-Veress, J.R. Dutcher, *Phys. Rev. E* **56**, 5705 (1997).
- J.A. Forrest, K. Dalnoki-Veress, J.R. Stevens, J.R. Dutcher, *Phys. Rev. E* **58**, 6109 (1998).
- J.R. Dutcher, K. Dalnoki-Veress, J.A. Forrest, in *Supramolecular Structure in Confined Geometries*, edited by G. Warr, S. Manne, *Am. Chem. Soc. Symp. Ser.* **736**, 127 (1999).
- J. Mattsson, J.A. Forrest, L. Börjesson, *Phys. Rev. E* **62**, 5187 (2000).
- K. Dalnoki-Veress, J.A. Forrest, C. Murray, C. Gigault, J.R. Dutcher, *Phys. Rev. E* **63**, 031801 (2001).
- J.A. Forrest, J. Mattsson, *Phys. Rev. E* **61**, R53 (2000).
- E. Hempel, G. Hempel, A. Hensel, C. Schick, E. Donth, *J. Phys. Chem. B* **104**, 2460 (2000).
- C.B. Roth, J.R. Dutcher, *Phys. Rev. E* **72**, 021803 (2005).
- C.B. Roth, J.R. Dutcher, to be published in *J. Polym. Sci., Part B: Polym. Phys.* (2006).
- Z. Fakhraai, S. Valadkhan, J.A. Forrest, *Eur. Phys. J. E* **18**, 143 (2005).
- P.G. de Gennes, *Eur. Phys. J. E* **2**, 201 (2000).
- P.G. de Gennes, *C. R. Acad. Sci. Paris, Sér. IV* **1**, 1179 (2000).
- D. Long, F. Lequeux, *Eur. Phys. J. E* **4**, 371 (2001).
- S. Merabia, P. Sotta, D. Long, *Eur. Phys. J. E* **15**, 189 (2004).
- S. Herminghaus, K. Jacobs, R. Seemann, *Eur. Phys. J. E* **5**, 531 (2001).
- S. Herminghaus, *Eur. Phys. J. E* **8**, 237 (2002).
- K. Ngai, *Eur. Phys. J. E* **8**, 225 (2002).
- K. Ngai, A.K. Rizos, *Mater. Res. Soc. Symp. Proc.* **455**, 147 (1997).
- C.J. Ellison, J.M. Torkelson, *Nature Mater.* **2**, 695 (2003).
- C.B. Roth, J.R. Dutcher, *Eur. Phys. J. E* **12**, s01, 024 (2003).
- The R_{ee} values were determined using data given in Table XXXIX of P.J. Flory, *Principles of Polymer Chemistry* (Cornell University Press, Ithaca, 1953) p. 618.
- We have not measured the tacticity content of the atactic PMMA, but an estimate of the relative isotactic and syndiotactic content can be obtained from the value of T_g^{bulk} . Higher T_g^{bulk} values indicate a higher percentage of syndiotactic content; PMMA with $T_g^{\text{bulk}} = 110^\circ\text{C}$ typically has a percentage of syndiotactic content of about 60%.
- R.M.A. Azzam, N.M. Bashara, *Ellipsometry and Polarized Light* (North-Holland Publishing Company, Amsterdam, 1977).
- No differences were observed in the measured T_g values if the sample chamber was flushed for 15 min with dry nitrogen gas instead of only 30 s.
- L.S.A. Smith, V. Schmitz, *Polymer* **29**, 1871 (1988).
- H. Shindo, I. Murakami, H. Yamamura, *J. Polym. Sci., Part A: Polym. Chem.* **7**, 297 (1969).
- S. Wu, *J. Phys. Chem.* **74**, 632 (1970).
- D.J. Plazek, K.L. Ngai, in *Physical Properties of Polymers Handbook*, edited by J.E. Mark (AIP, Woodbury, NY, 1996) Chapt. 12.
- K.K. Chee, *J. Appl. Polym. Sci.* **43**, 1205 (1991).
- X.Y. Lu, B.Z. Jiang, *Polymer* **32**, 471 (1991).
- The possibility of a larger energy barrier for de Gennes' sliding mode for PMMA relative to that for PS is supported by the observation that, at 100°C , the monomeric friction coefficient ζ is $\sim 50\%$ greater for PMMA than for PS, see G.C. Berry, T.G. Fox, *Adv. Polym. Sci.* **5**, 261 (1968).
- R. Subramanian, R.D. Allen, J.E. McGrath, T.C. Ward, *Polymer Prepr.* **26**, 238 (1985).
- J.M. O'Reilly, R.A. Mosher, *Macromolecules* **14**, 602 (1981).
- Y. Grohens, R.E. Prud'homme, J. Schultz, *Macromolecules* **31**, 2545 (1998).
- P.R. Sundararajan, *Macromolecules* **19**, 415 (1986).
- M. Vacatello, P.J. Flory, *Macromolecules* **19**, 405 (1986).
- K. Schmidt-Rohr, A.S. Kulik, H.W. Beckham, A. Ohlemacher, U. Pawelzik, C. Boeffel, H.W. Spiess, *Macromolecules* **27**, 4733 (1994).
- S.C. Kuebler, D.J. Schaefer, C. Boeffel, U. Pawelzik, H.W. Spiess, *Macromolecules* **30**, 6597 (1997).